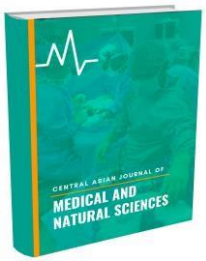

CENTRAL ASIAN JOURNAL OF MEDICAL AND NATURAL SCIENCES
https://cajmns.centralasianstudies.org/index.php/CAJMNS
Volume: 05 Issue: 04 | October 2024 ISSN: 2660-4159

Article

The Value of Combination of Diffusion-Weighted Sequences and Dynamic Contrast MRI Study in Differentiation between Benign and Malignant Breast Lesions

Sarah Ghaleb Shati[1]

1. Lecturer, M.B.Ch.B., C.A.B.M.S., Diagnostic Radiology, Ministry of Higher Education and Scientific Research, Department of Surgery, College of Medicine, University of Thi-Qar, Thi-Qar, Iraq

* Correspondence: sarahghalib@utq.edu.iq

Abstract: MRI, as defined, is a diagnostic imaging technique that employs the use of magnets and high-powered radio waves to analyses the internal structures of the body. The evaluation of breast tumours and the description of lesions that are not adequately observed by mammography or ultrasound. The objective of this study was to evaluate the diagnostic accuracy of DW-MRI and ADC value in differentiating between benign and malignant breast lesions when combined with dynamic contrast-enhanced MRI. A prospective analytic study was conducted on a cohort of women attending the MRI unit of the Radiology Department at Al-Imamein Al-Kadhimein Medical City in Baghdad between April 2018 and February 2019. All women were enrolled in the study prior to undergoing a biopsy, during which dynamic contrast-enhanced (DCE) MRI and diffusion-weighted imaging (DWI) were performed. The image fusion of DCE-MRI with the apparent diffusion coefficient (ADC) map was employed to identify the region of interest (ROI) for ADC calculation in the area that demonstrated the most avid enhancement. DWI was acquired at the following b-values (0, 400, 800 sec/mm^2). The mean age of the 38 patients was (39.83 ± 10.476) years, with a range of (16-62 years). Of the 46 lesions, 20 (43.5%) were identified as malignant, while 26 (56.5%) were classified as benign. The mean ADC value of all benign lesions was 1.585 ± 0.182 x 10^{-3} mm^2/s, which was higher than the mean ADC of all malignant lesions (1.149 ± 0.214 x 10^{-3} mm^2/s) (P < 0.0001). Furthermore, a notable distinction was observed between mass and non-mass-enhanced lesions in terms of mean ADC values. The mean ADC value for benign mass lesions was found to be (1.538 ±0.147 x10-3 mm^2/s), while the mean ADC value for benign non-mass enhanced lesions was (1.785 ±0.087 x10-3 mm^2/s). This difference was statistically significant (P-value 0.004).

Keywords: DCE, DWI, MRI, ADC, Breast, Benign breast lesion, Malignant breast lesion

Citation: Shati, S. G. The Value of Combination of Diffusion-Weighted Sequences and Dynamic Contrast MRI Study in Differentiation between Benign and Malignant Breast Lesions. Central Asian Journal of Medical and Natural Science 2024, 5(4), 627-635.

Received: 8th Aug 2024
Revised: 15th Aug 2024
Accepted: 22nd Aug 2024
Published: 29th Aug 2024

1. Introduction

The adult breast is situated on the front side of the chest wall and is upheld by Cooper's ligaments. The breast is composed of adipose and fibro-glandular tissue, with the nipple-areola complex located at its core. The breast consists of 15-18 lobes, with each lobe comprising 20-40 lobules [1, 2]. The terminal ductal lobular unit (TDLU) is the fundamental functional unit of the breast. It is composed of 10-100 acini that empty into the terminal duct, which in turn empties directly into the nipple [3, 4, 5]. Constriction of these cords might result in skin indentation. The detection of breast cancer has undergone substantial advancements since the early 20th century, primarily due to the emergence of advanced mammography and ultrasound imaging techniques [6, 7, 8]. Nevertheless, because there

is an overlap in characteristics between benign and malignant tumors, standard MRI features may lack the ability to distinguish between them where DWI computes the apparent diffusion coefficient (ADC), which is directly linked to the diffusion of water in tissues. Malignant lesions exhibit a lower apparent diffusion coefficient (ADC) value as a result of their increased cellular density, bigger nuclei, and diminished extracellular space [9, 10, 11, 12].

Lymphatic drainage in breasts occurs from deep breast tissues to superficial lymphatics and peri areolar lymphatic plexus. 75% of drainage occurs through lateral and medial trunks, while 25% is carried out by internal mammary nodes [13, 14, 15]. Axillary lymph nodes are organized into levels, and lymph nodes can also be found within breast tissue [16, 17]. Near the internal mammary veins, and surrounded by extra pleural fat in a parasternal position [18, 19, 20]. Throughout the typical lifespan, there are alterations in the makeup of glandular breast tissue and stroma. Younger women possess a greater amount of glandular tissue, whereas older women possess more fatty tissue. Hormone replacement therapy prolongs the preservation of glandular breast tissue.

2. Patients and Methods

In order to assess the Histo-pathological results of 46 breast lesions in patients and to understand the conclusion from ADC values (x10-3 mm^2/s) for benign and malignant breast lesions in patients. When used in conjunction with dynamic contrast-enhanced MRI. The study included 38 women who had ambiguous or worrisome breast tumors identified using ultrasonography or mammography. The exclusion criteria encompassed contraindications to MRI examination, reluctance to participate, inability to assume a prone posture, pregnancy, BIRAD I and II classifications, and prior biopsy. Data regarding demographic parameters, clinical history, and imaging findings were gathered.

The study included participants who underwent an MRI examination utilizing a 1.5 Tesla MR Unit equipped with bilateral sixteen-channel breast coils. Where in this study, we included examination (axial T1 weighted images, axial T2 weighted images, axial T2 fat suppression weighted images, diffusion-weighted images) and a dynamic T1 post-contrast fat-suppressed image. The ADC map was automatically generated within the MR system. In the dynamic magnetic resonance (MR) investigation, Gd-DTPA was administered intravenously via an automated injector. The patient assumed a prone position, with the breast resting on the coil and the nipples facing downwards in a stationary manner.

Radiologists utilized the BI-RADS breast MRI lexicon to perform breast imaging and histopathology. Every lesion was detected in T1, T2, and T2 fat suppression weighted images, as well as dynamic subtracted pictures. Dynamic MR images were used to produce time-signal intensity curves. The types of lesions were characterized based on their morphology, margin, and internal enhancement patterns.

The study received approval from the local scientific committee of the Arab Board of Medical Specialization, and patients supplied oral agreement after being told about the study. The data was analyzed using SPSS version 22, employing several contingency tables and statistical tests such as the Chi-square test. The study also evaluated the sensitivity, specificity, and accuracy of DCE-MRI and DWI, with a statistically significant P-value of less than 0.05.

3. Results

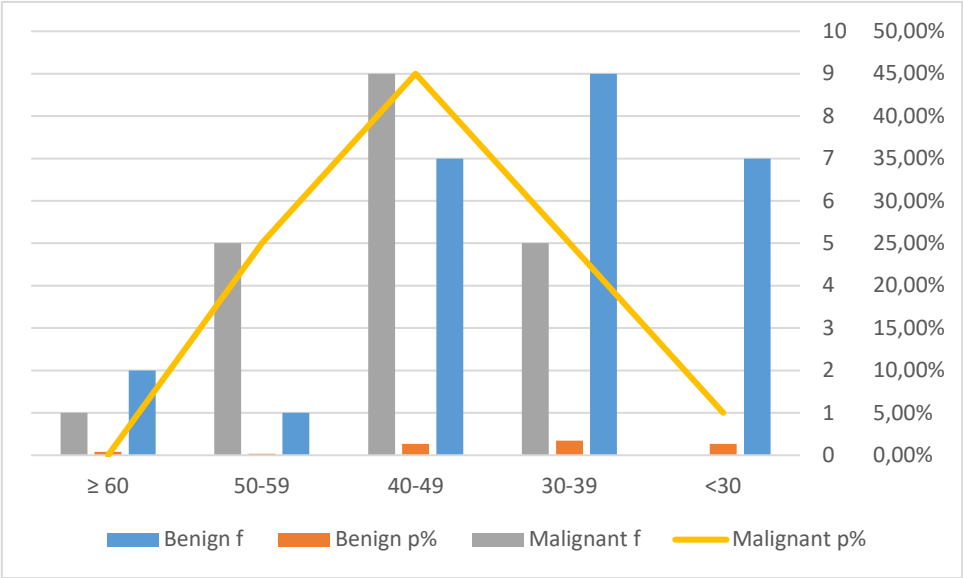

Figure 1. Age distribution for malignant and benign lesions among the patients

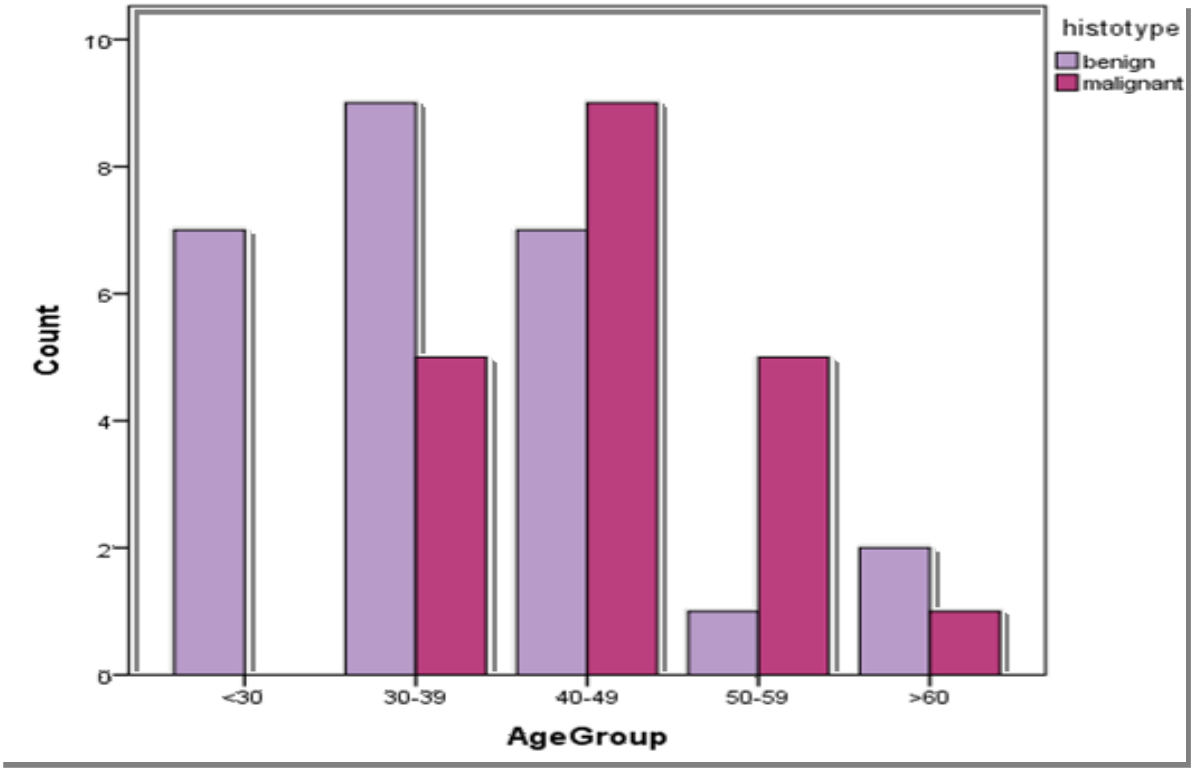

Figure 2. Age distribution of patients with malignant and benign tumors

Table 1. Lesion types in relation to histopathological results among the patients

	Benign		Malignant		P-value
Mass	21	80.8%	13	65%	
NME	5	21.7%	7	35%	0.22
Total	26	100.0%	20	100.0%	

Table 2. Distribution of NME lesions and histopathological results among the patients

	Benign		Malignant		P-value
Segmental	0	0%	2	28.6%	
Linear	2	40.0%	3	42.8%	
Regional	2	40.0%	0	0%	0.39
Focal	1	20.0%	2	28.6%	
Total	5	100.0%	7	100.0%	

Table 3. Shape of mass lesion in relation to histopathological reports among patients

	Benign		Malignant		P-value
Rounded	14	66.7%	7	53.8%	
Oval	7	33.3%	0	0.0%	
Irregular	0	0.0%	6	46.2%	<0.03*
Total	21	100.0%	13	1 00.0%	

Table 4. Margin of mass lesions in relation to histopathological results

	Benign		Malignant		P-value
well-circumscribed	21	100.0%	0	0.0%	
Irregular	0	0.0%	6	46.2%	<0.0001*
Spiculated	0	0.0%	7	53.8%	
Total	21	100.0%	13	100.0%	

Table 5. Type of internal enhancement pattern of lesions with histopathological results

	Benign		Malignant		P-value
Homogenous	12	46.2%	0	0%	
Heterogeneous	8	30.8%	11	55.0%	
Rim-enhancement	0	0%	6	30.0%	
Central	3	11.5%	0	0%	<0.0001*
non-enhanced septa	3	11.5%	0	0%	
Clumped	0	0%	3	15%	
Total	26	100.0%	20	1 00.0%	

Table 6. Type of curve in relation to histopathological reports among the patients

	Benign		Malignant		Total
Curve Type I	15	83.3%	3	16.7%	18
Curve Type II	9	56.25%	7	43.75%	16
Curve Type III	0	0.0%	10	100%	10
P-value	<0.0001*				

*The result was significant at a P-value <0.05.

Table 7. The histopathological results of 46 breast lesions among the patients

Result of the Histopathology		**No.**	**%**
Benign		26	56.5%
Malignant		20	43.5%
Benign	Fibroadenoma	18	39.1%
	Fibrocystic	4	8.7%
	Fat necrosis	2	4.3%
	Mammary adenosis	1	2.2%
	Benign phylloid	1	2.2%
Malignant	Ductal	13	28.3%
	DCIS	2	4.3%
	Lobular	3	6.5%
	Lobular insitu	2	4.3%

Table 8. Assessment distribution according to ADC

	Benign	**Malignant**	**P-value**
Mean±SD	1.585±0.182	1.149±0.214	<0.0001*
Range	1.330-1.950	0.6-1.480	

4. Discussion

The research study identified a total of 46 lesion sites across 38 patients with an age distribution ranging from 16 to 62 years old. The most frequent age was 16 to 60 years ago group in which 7 cases were recorded out of 38 samples analyzed.

A total of 46 lesions were identified. Of the total number of lesions, 34 were classified as mass enhancement (ME) and 12 as non-mass enhancement (NME). Upon histopathological examination, 26 were identified as benign and 20 as malignant.

Of the benign lesions, 21 (80.8%) were of the mass type, while 5 (21.7%) were of the non-mass enhancement (NME) variety. Of the malignant lesions, 13 (65%) were masses, and 7 (35%) were non-mass enhancement (NME). As illustrated in Table 3-2, 24 patients exhibited a solitary mass lesion, six patients presented with an NME lesion, six patients displayed a combined mass and NME lesion, and two patients demonstrated multiple lesions comprising two masses.

The multiple lesions were as follows: two patients presented with two benign masses (fibroadenoma), three patients exhibited a combined malignant mass and NME (ductal carcinoma in situ), one patient displayed a benign NME plus malignant mass (fibrocystic plus ductal carcinoma in situ), and two patients demonstrated a combined benign NME (fibrocystic/adenosis) associated with a benign mass (fibroadenoma).

The study found that the average size of the mass lesions was 25.24±8.61 mm, with the smallest lesion being 10 mm. The Pearson correlation coefficient between the ADC value and the variable of interest is 0.065, with a corresponding P-value of 0.7.

With respect to histology, the mean ± standard deviation for the malignant lesions' mass size was (23.38± 9.37 mm) while that of their benign counterparts was (26.38± 8.12 mm). The size of the mass lesion was not correlated with histopathological findings, as shown by p = 0.41.

Regarding histology, the average ± standard deviation size of the malignant lesions' mass was (23.38± 9.37 mm), and for benign lesions' mass was (26.38± 8.12 mm) with a p-value of 0.41

Two non-mass enhancing lesions were segmental, with 28.6% being malignant, while linear and focal patterns were found in five and three lesions, respectively, with varying proportions of malignancy. Result Set Rs = someStmt. Execute Query: However, none of this information had any statistical significance (P>0.05).

A total of twenty-one rounded lesions were identified (fourteen with benign histology, representing 66.7%, and seven with malignancy, representing 53.8%). Oval was the shape of seven of them, with one-third that were benign, and of the six remaining, some were irregular, with more than a forty-six percent likelihood of being cancerous. Those were significant findings at P=0.03 or less.

In terms of the margin of mass lesions, there were 21 that were well-circumscribed (all of which were benign, accounting for 100% of benign lesions), 6 with irregular margins (all of which were malignant, representing 46.2% of all malignant lesions), and seven that were spiculated (all of which were malignant, accounting for 53.8% of all malignant lesions). These findings had a significant P-value.

In terms of enhancement patterns, 55% of the malignant lesions displayed a heterogeneous pattern, 30% showed a rim pattern, and 15% had a clumped pattern. On the other hand, 46.2% of the benign lesions exhibited a homogeneous pattern, 30.8% were heterogeneous, 11.5% had a central pattern, and 11.5% had non-enhancing septa. Having a P-value of less than 0.0001, which is extremely significant.

Regarding the curves observed on DCE-MRI, type I (permanent) was found in 18 lesions, with 13 being benign (83.3%) and three being malignant (16.7%).

The study observed a Type II (plateau) enhancement pattern in 16 lesions, with 10 of them being benign (40.9%) and seven malignant (36.8%). Additionally, a Type III (washout) enhancement pattern was found in 10 malignant lesions, where the finding was statistically significant with a P-value of <0.0001. Out of the total of 26 benign lesions, 15 (62.5%) were classified as curve type I, while 9 (37.5%) were classified as curve type II. There were no lesions classified as curve type III. Out of the 20 malignant lesions, 3 (15%) were classified as curve type I, 7 (35%) as curve type II, and 10 (50%) as curve type III. Nevertheless, there were two lesions (NME) with an undependable curve type.

Out of the total of 20 malignant lesions, 13 (28.3%) were classified as ductal carcinoma, 2 (4.3%) were classified as ductal carcinoma in situ, 3 (6.5%) were classified as lobular carcinoma, and 2 (4.3%) were classified as lobular carcinoma in situ.

Out of the total 26 benign lesions, 18 (56.5%) were fibroadenoma, 4 (39.1%) were fibrocystic alterations, 2 (8.7%) were fat necrosis, 1 (4.3%) was mammary adenosis, and 1 (2.2%) was benign phylloid.

The ADC values for benign lesions ranged from 1.330 to 1.950 x10-3mm2/s, while for malignant lesions, it ranged from 0.600 to 1.480 x10-3mm2/s.

A statistically significant difference (P-value <0.0001) was detected between the mean ADC values for malignant (1.149±0.214x10-3 mm^2/s) and benign (1.585±0.182 x10-3 mm^2/s) lesions.

The assessment of breast lesions on MRI is dependent on the morphological criteria, the T2 characteristics of the lesions, and the pattern of enhancement kinetics. The characterisation of discovered lesions can prove challenging due to the significant similarities in imaging criteria between malignant and benign lesions. Furthermore, the accuracy of characterisation is contingent upon the expertise of the reader, resulting in significant interobserver variability in interpretation.

The implementation of supplementary criteria for the characterization of worrisome lesions has the potential to effectively reduce the number of invasive breast surgeries. Diffusion-weighted imaging (DWI) utilises the microscopic, thermally-generated, random movement of molecules, which is commonly referred to as Brownian motion. The quantification of DWI is based on the measurement of apparent diffusion coefficient (ADC) values. However, there is a convergence between these two entities since benign breast tumours can exhibit low ADC levels and simulate malignancies.

5. Conclusion

The current classification of breast cancer (BC) is based on its genetic or molecular characteristics, which fall into three main groups. These groups have different implications for diagnosis and treatment. The role of magnetic resonance imaging (MRI) in the diagnosis and staging of breast cancer (BC), in planning surgical treatment, and in screening high-risk patients is well established. Furthermore, it is important to emphasise that the assessment of response to primary systemic therapy (PST) is one of the most accepted assessments within the recommendations for the use of breast MRI set forth by the European Association of Breast Cancer Specialists. This assessment is supported by level of evidence type 1 and level of recommendation A2.

The advent of new technology has enabled MRI to advance from a diagnostic tool to one that can also provide insights into molecular characteristics, thereby forming the foundation for the selection of targeted therapy.

REFERENCES

[1] E. Morris and L. Liberman, *Breast MRI*, New York, NY, USA: Springer, 2004.

[2] D. Thigpen, A. Kappler, and R. Brem, "The Role of Ultrasound in Screening Dense Breasts-A Review of the Literature and Practical Solutions for Implementation," *Diagnostics (Basel)*, vol. 8, no. 1, p. 20, 2018.

[3] U. Sharma, R. G. Sah, and K. L. Agarwal, "Potential of Diffusion-Weighted Imaging in the Characterization of Malignant, Benign, and Healthy Breast Tissues and Molecular Subtypes of Breast Cancer," *Frontiers in Oncology*, vol. 6, pp. 128-134, 2016.

[4] Y. Gordon, S. Partovi, and M. Müller-Eschner, "Dynamic Contrast-Enhanced Magnetic Resonance Imaging: Fundamentals and Application to the Evaluation of the Peripheral Perfusion," *Cardiovasc Diagn Ther.*, vol. 4, no. 2, pp. 147-164, 2014.

[5] S. Sinha and U. Sinha, "Functional Magnetic Resonance of Human Breast Tumors: Diffusion and Perfusion Imaging," *Ann. N.Y. Acad. Sci.*, vol. 980, pp. 95-115, 2002.

[6] S. Partridge, N. Nissan, H. Rahbar, A. Kitsch, and E. Sigmund, "Diffusion-Weighted Breast MRI: Clinical Applications and Emerging Techniques," *Journal of Magnetic Resonance Imaging*, vol. 45, no. 2, pp. 337-345, 2016.

[7] T. Imamura, I. Isomoto, E. Sueyoshi, H. Yano, T. Uga, and K. Abe, "Diagnostic Performance of ADC for Non-Mass-Like Breast Lesions on MR Imaging," *Magn Reson Med Sci.*, vol. 9, pp. 217-225, 2010.

[8] H. Hassan, M. Mahmoud Zahran, H. El-Prince Hassan, A. Mohamed Abdel-Hamid, and G. Abdel Shafy Fadaly, "Diffusion Magnetic Resonance Imaging of Breast Lesions: Initial Experience at Alexandria University," *Alexandria Journal of Medicine*, vol. 49, pp. 265-272, 2013.

[9] S. Tan, K. Rahmat, F. Rozalli, M. Mohd-Shah, Y. Aziz, C. Yip, *et al.*, "Differentiation Between Benign and Malignant Breast Lesions Using Quantitative Diffusion-Weighted Sequence on 3 T MRI," 2014, vol. 54, pp. 67-73.

[10] P. Butler, A. Mitchell, and H. Ellis, *Applied Radiological Anatomy for Medical Students*, 1st ed., Cambridge, UK: Cambridge University Press, 2007, p. 31.

[11] S. Ryan, M. McNicholas, and S. J. Eustace, *Anatomy for Diagnostic Imaging*, 3rd ed., Edinburgh, UK: Baillière Tindall, Elsevier, 2011.

[12] R. G. Grainger, D. J. Allison, A. K. Dixon, *et al.*, *Grainger & Allison's Diagnostic Radiology: A Textbook of Medical Imaging*, 6th ed., Edinburgh, UK: Churchill Livingstone/Elsevier, 2015.

[13] L. Glassman and M. Hazewinkel, "The Radiology Assistant: Breast – MRI," *Radiology Assistant*, 2009. [Online]. Available: http://www.radiologyassistant.nl/en/p47a585a7401a9/breast-mri.html. [Accessed: Dec. 30, 2017].

[14] D. Ikeda and K. Miyake, *Breast Imaging*, St. Louis, MO, USA: Mosby, 2016.

[15] W. A. Berg and W. T. Yang, *Diagnostic Imaging: Breast*, Salt Lake City, UT, USA: Amirsys, 2014.

[16] C. J. Dorsi, E. B. Mendelson, and D. M. Ikeda, *ACR Breast Imaging and Reporting Data System: Breast Imaging Atlas*, Reston, VA, USA: American College of Radiology, 2013, vol. 76, no. 32, pp. 234-242.

[17] G. Cardenosa, *Clinical Breast Imaging: The Essentials*, Philadelphia, PA, USA: Wolters Kluwer, 2015.

[18] W. Hetta, "Role of Diffusion-Weighted Images Combined with Breast MRI in Improving the Detection and Differentiation of Breast Lesions," *Radiology*, vol. 46, no. 2, pp. 259-270, 2015.

[19] C. K. Kuhl, R. Schmutzler, and C. C. Leutner, "Breast MR Imaging Screening in 192 Women Proved or Suspected to Be Carriers of a Breast Cancer Susceptibility Gene: Preliminary Results," *Radiology*, vol. 215, pp. 267-279, 2000.

[20] Y. Ibrahim, L. Habib, and A. Deif, "Role of Quantitative Diffusion-Weighted Imaging in the Characterization of Breast Masses," *Radiology*, vol. 46, pp. 805-810, 2015.